INVESTIGATION OF THE FLUID MECHANICAL BEHAVIOR OF A THERMAL STORAGE RESERVOIR FOR DRY-COOLED CENTRAL POWER STATIONS

E.C. Guyer and M.W. Golay
Massachusetts Institute of Technology
Cambridge, Massachusetts U.S.A.

ABSTRACT

The use of a capacitive Thermal Storage Pond (TSP) initially filled with cold water as part of a dry cooling system for a central power station is attractive economically if the pond can be designed to operate in an approximate "plug-flow" mode-discharging cold water to the condenser and filling with hot water from the cooling tower. Bouyant flow stratification hinders attaining this goal since it can cause "short circuiting" of the pond. For adequate flow control, a long narrow pond configuration (possibly serpentine) is desirable. In investigating the behavior of such a pond experimentally, it was found over the range of cases examined that injection of water into a long narrow reservoir which is initially at a different temperature always results in a stratified flow, which could be modelled analytically successfully in terms of a static "lock-exchange" type flow superimposed upon the gross plug flow of the pond. Such behavior is undesirable in a TSP, and it was found that acceptable performance could be obtained inexpensively by placing flow-constricting barriers at regular intervals along the pond length.

INTRODUCTION

The combined thermal storage pond (TSP) and dry cooling tower system concept is proposed as a solution to performance problems of dry cooled central power stations. [1] Simple dry-cooling of a steam-electric plant results in severe economic penalties due to the coincidental occurrence of the daily period maximum loss of electrical generation capability resulting from high condenser temperatures and the daily period of maximum utility system electrical demand. The daily maximum condenser temperature would occur during the afternoon period of peak electrical demand since the ambient dry bulb, which is normally at a maximum during the early afternoon, is directly reflected in the steam condensing temperature for dry cooling systems. The combined thermal storage pond and dry cooling tower system represents an attempt to avoid this undesirable coincidental occurrence of the maximum ambient temperature and the maximum electrical demand through the cyclic operation of the TSP and dry tower system. The combined system is operated such that condenser temperature during the afternoon period approaches

the daily minimum ambient temperature occurring in the early morning rather than the daily maximum ambient temperature occurring in the afternoon. Economic analysis of this system has indicated substantial economic benefit in taking advantage of the 30°F or greater daily range of the ambient temperature common to many of the western regions of the United States [2].

The cyclic operation of the combined TSP and dry tower system encompasses four operational modes. They are the following:

1) cold standby mode,

2) heatup mode,

3) hot standby mode, and

4) cooldown mode

The cold standby mode would normally be utilized during the late morning hours; in this mode the condenser is cooled solely by the dry cooling tower. However, during the heatup operational mode period, the period of maximum ambient temperature and maximum electrical demand, relatively cool water would be drawn from the pond, passed through the condenser and dry cooling tower, and then would be discharged back into the pond at an increased temperature. When the cooling potential of the pond had been exhausted or the afternoon period of peak electrical demand had passed, the system would be switched to the hot standby mode, which is essentially identical to the cold standby mode of operation. Then when the ambient temperature had declined to near its daily minimum value the coupling of the pond with the condenser and dry tower again would occur. During this final mode of operation, the cooldown mode, relatively warm water would be drawn from the pond, passed through the condenser and dry tower, and discharged back into the pond at a relatively cool temperature.

Once the entire volume of the pond had been recooled, the daily cycle would be repeated.

The basic function of a thermal storage pond is thus to provide simultaneously a condenser cooling water source and a holding facility for the same water after it has passed through the condenser and has been recooled partially by the dry cooling tower. The type of thermal-hydraulic behavior required in the pond is exactly that of the well-known plug-flow. However, exact plug-flow in the pond may not be required since the dry cooling tower/TSP system may still perform effectively - in an economic sense - in spite of some undesirable mixing of hot and cold water in the pond. The extreme case of mixing of the initial pond inventory with incoming flow is the case of

fully-mixed behavior. A further limit beyond that of the idealized fully-mixed case - in terms of overall system performance degradation - is that of the short-circuited pond. This situation is highly undesirable since any fraction of the pond which is isolated from the flow circuit becomes lost as a medium for the storage of waste heat with the net result that the effective storage volume of the pond is reduced accordingly.

The work reported herein summarizes the analytical and experimental investigation which was undertaken in an effort to formulate a preliminary TSP design which would result in a good approximation to the desired plug-flow behavior. As is indicated in the following discussion, an economically practical design has been achieved.

Design Constraints and Requirements

In attempting to formulate some preliminary design options for the plug-flow TSP it was necessary to consider the engineering and economic constraints or requirements which will be imposed on any design concept. A list of some of the desirable features of a well-designed pond is the following:

1) low pond head loss during operation,

2) low pond flow velocity,

3) minimal bottom and surface area,

4) avoidance of excessive depth,

5) smooth response of the TSP outlet temperature to changes in the inlet temperature,

6) effective operation during both "heatup" mode and "cooldown" mode of operation, and

7) modest inlet flow velocities.

The requirement of low pond head loss during operation stems simply from the fact that during the standby stage of the TSP operation the surface elevation of the pond will seek its natural level. If the pond structure must also contain the extra water elevation due to a large head loss through the flow circuit of the pond then storage capacity will be wasted. A low pond flow velocity is also desirable since the pond lining and covering will likely be fabricated from flexible plastic or rubber membranes.

The requirements of minimal bottom and surface areas and

reasonable depth are contradictory when attempting to design a TSP for a fixed storage volume. Thus, some compromise is required. Minimal surface area is desirable for either the open or covered pond. In the case of the open pond it is of interest to minimize evaporation, and in the case of the covered pond it is of interest to minimize the cost of covering and lining the structure. The need to maintain a reasonable depth is connected with the difficulty of constructing high dikes for an above-ground level pond, and of excavating to large depths for a below ground level pond.

Additionally, it is a basic design requirement that the TSP outlet temperature respond smoothly to the inlet temperature. Large and high frequency variations in the TSP outlet temperature (condenser temperature) as the storage capacity of the pond nears exhaustion could result in unacceptable transients in the turbine-generator behavior.

A most fundamental requirement is that the TSP function effectively during both the "heatup" and "cooldown" modes of operation. Designing for one mode of operation will not automatically result in a correct design for the other due to the potential for the occurrence of density-induced stratified flows in the TSP.

Finally, it is desirable to minimize the inlet velocity into the pond since the velocity head of the inlet flow is non-recoverable and requires an additional amount of circulating water pumping power above that required for the operation of the tower only.

Feasible Solutions to the TSP Design Problem

There are two general methods by which the desired plug-flow behavior may be achieved. They are by means of horizontal plug-flow and vertical plug-flow. Figure 1 schematically demonstrates how the two types of behavior might be obtained in situations in which the reservoir is being filled with warm water. In the vertical plug-flow case one would attempt to take advantage of the tendency for stable vertical stratification, and in the case of the horizontal plug-flow one would have to guard against the tendency for vertical stratification (with the warm water floating above the colder water).

Both the vertical and horizontal plug-flow design options have particular advantages and disadvantages with regard to the previously discussed economic and engineering constraints and performance requirements. Based on a comparison of the two options it was decided that an attempt would be made to design a horizontal plug-flow pond.

The major concern in the design of a horizontal plug-flow TSP was identified as being the instability of an initially vertical front across which large density differences would exist. The presence of the density difference across a vertical interface will give rise to density-induced flows which could be a significant factor in determining the thermal efficiency of the TSP. The ratio of the rate of propagation of the density front due to the nominal plug-flow velocity in the TSP to the rate of propagation of the density front due to density-induced flows can, in a general fashion, be characterized by the densimetric Froude number of the TSP. The TSP densimetric Froude number is given as

$$F_d = \frac{V_p}{\sqrt{\frac{\Delta\rho}{\rho} gH}} \qquad (1)$$

where $\Delta\rho$ = the density difference

ρ = average density,

H = pond depth,

g = gravitational acceleration, and

V_p = plug-flow velocity

Designing the TSP for a large densimetric Froude number should result in the nominal plug-flow velocity dominating the density-induced currents. At the extreme of very large design densimetric Froude numbers near-perfect horizontal plug-flow should result as shown in Fig. 1. However, large design densimetric Froude numbers also result in high TSP construction costs since a narrow, shallow, and long pond structure is required.

It was from this realization that the fundamental fluid mechanical design task became apparent - the specification of the minimal design densimetric Froude number such that an acceptable level of performance is achieved.

To provide the required ability to describe the behavior of a propagating density front in a horizontal plug-flow TSP a control-volume type fluid dynamic model has been derived, and its predictions have been compared to experimental results. The experiment has been designed such that it serves the dual purposes of providing the data necessary to construct the semi-empirical mathematical model of transient stratified flow in shallow channels for a limited range of densimetric Froude

numbers, and of providing a physical model of a prototype thermal storage pond.

PHYSICAL MODEL

Similarity Requirements

Total physical similarity between model and prototype TSP's requires similarity of flow in three regions. These are the entrance mixing region, the main storage volume, and the withdrawal region. The intent in physically modeling a horizontal plug-flow TSP is the replication of the behavior of the entrance mixing and main storage regions. Modeling of the withdrawal region is not crucial in this work, since if the horizontal plug-flow concept is to be viable, vertical stratification in the withdrawal region will necessarily be minimal.

Similarity to the entrance region of a prototype TSP is obtained in the model in an integral sense by assuming that any submerged jet discharge with a highly unstable near-field region will produce essentially the same vertical temperature mixing effect in a geometrically similar region, without regard for the geometrical details of the discharge structures. Since the volume of the entrance region is small in relation to the total storage volume this assumption is observed experimentally to be adequate. In both the model and the prototype an unstable near-field flow can be obtained by using a horizontal multiport submerged jet discharge with the jets uniformly spread over the width of the pond.

To insure similarity between the main storage volume flows of the model and the prototype, the following requirements are met:

1) geometric similarity,

2) Froude Law similarity,

3) densimetric Froude Law similarity,

4) satisfaction of the turbulent flow Reynolds criterion, and

5) similarity of the ratio of inertial to friction forces.

In Froude models it is impossible to meet both Froude similarity and Reynolds similarity exactly. However, exact similarity of Reynolds number for turbulent flows is not required. It is generally satisfactory to meet the criterion

$$Re_{model} > Re_c$$

where Re_c is the critical Reynolds number for fully developed turbulent flow.

Although it is not essential to meet Reynolds number similarity, it is important, as noted by Jirka (2) that the ratio of inertial forces to bottom friction forces be equal for the model and the prototype. Thus in the physical modeling of the prototype TSP it is desirable to distort the vertical dimension of the model such that the ratio of friction forces to inertial forces in the prototype is approximately replicated in the model.

Experimental Apparatus and Observational Techniques

The experimental model of the prototype TSP has been constructed at the Ralph M. Parsons Laboratory for Water Resources and Hydrodynamics at M.I.T. The model fabrication consisted mainly of the modification of an existing flume. The flume is constructed of 1/2" glass mounted on an aluminum frame. The nominal flume dimensions are 8" deep, 18" wide and 64 feet long. The piping and storage tanks which were added to the facility to enable the desired inlet discharge and withdrawal flowrates to be maintained in the model are shown schematically in Fig. 2.

As is indicated in Fig. 2, a flume recirculation line was installed to allow the initial pond inventory to be continuously cycled through the flume in order to diminish any temperature differences which may develop just prior to the actual experiment. Also the recirculation flow allows the plug flow velocity field to be established in the flume prior to the introduction of hot inlet water. The inlet and withdrawal flow rates are measured by rotor-meters with maximum capacities of 67 gpm. The inlet discharge structure consists of four 2 in. nozzles which could be reduced in size. Various withdrawal schemes were utilized during different experimental runs depending on the current modeling requirements.

The flow visualization dye, FD+C Blue Food Color #1, was used to color the entire contents of the inlet flow holding tank just prior to the operation of the experiment. Simple visual recording of the position of the density front at known instants was acceptable for recording the bulk fluid behavior. Thermistors with short response times were used to record the transient temperatures at the point of withdrawal.

Analytical Model

An approximate analytical model of the behavior of a density front in a horizontal plug-flow pond has been developed based on a control-volume momentum conservation equation. The resultant equation contains one empirical constant, the value of which is determined by experiment. Essentially the model utilizes the superposition of the density-induced "lock-exchange" flow field upon the unperturbed homogenous fluid velocity profile in the pond. It includes interfacial and bottom friction effects.

The equation of motion of the leading and trailing edges of the density front in a horizontal plug-flow pond is obtained from a force balance on the double-lumped moving control volume shown in Fig. 3. The forces affecting the motion of the leading and trailing edges of the density front with respect to the mean plug-flow velocity V_p are the following:

1) F_p = pressure force due to $\rho_2 > \rho_1$,

2) F_i = interfacial friction force,

3) F_b = bottom friction force, and

4) F_m = inertial force, where

F_i, F_b, and F_m all act to resist the pressure force F_p. Thus, one obtains the result

$$F_p = F_i + F_b + F_m \quad . \qquad (2)$$

The approximate analytic expression for V_f, the leading edge velocity, and V_t, the trailing edge, is obtained by expressing Eq. (2) in terms of $\frac{dD}{dt}$, the rate of growth of the horizontal interfacial length. Thus, under the assumption of equal depths of the two overlying layers, and from the requirement of continuity one obtains the result

$$V_f - V_p = V_p - V_t = \frac{dD}{dt}/2 \quad . \qquad (3)$$

The total static pressure due to density difference acting horizontally across any point on the interface is

$$(P_2 - P_1)h = h\,(\rho_1 - \rho_2)\,\frac{g}{g_c} \qquad (4)$$

where h is the depth into the pond.

Since this pressure difference is a linear function of depth the total pressure acting across the interface is given as

$$\frac{(P_2 - P_2)}{2} \quad HA \tag{5}$$

where $(P_2 - P_1)$ is the pressure difference at the bottom of the pond, and A is the cross-sectional area of the pond, (A = L·H, where L = width). The average pressure can be envisioned to act to the right on the top fluid segment in the control volume and to the left on the bottom fluid segment. Substitution of Eq. (4) into Eq. (5) gives the result

$$F_p = \frac{\beta}{2} LH^2 \Delta\rho \frac{g}{g_c} \quad , \tag{6}$$

where the parameter β has been introduced to account for the fact that the actual pressure difference may be different from that deduced from the simple model.

The friction force terms in Eq. (2) can be expressed as

$$\begin{aligned} F_i &= \tau_i A_i, \text{ and} \\ F_b &= \tau_b A_b \end{aligned} \tag{7}$$

where $A_i \simeq A_b = D \cdot L$, and τ_i and τ_b are the interfacial and bottom shear forces, respectively. The interfacial shear is given by

$$\tau_i = \frac{f_i}{8} \rho V_R^2 = \frac{f_i}{8} \rho \left(\frac{dD}{dt}\right)^2 \quad . \tag{8}$$

where f_i is the interfacial friction factor. The variation of F_i with Reynolds number has been deduced by Abraham and Eysink (3).

The bottom shear force will be effected by the magnitude of the plug-flow velocity. The resultant bottom shear force is

$$\tau_b = \frac{f_b}{8} \rho \left(\left(\frac{dD}{dt}\right) \frac{V_p}{2} - \frac{1}{4} \left(\frac{dD}{dt}\right)^2 \right) . \tag{9}$$

The inertial force acting on the control volume is

$$F_m = \frac{d(M\bar{V})}{g_c dt} \quad , \tag{10}$$

or

$$F_m = \frac{M}{g_c} \left(\frac{d\bar{V}}{dt}\right) + \frac{\bar{V}}{g_c} \frac{dM}{dt} \quad , \tag{11}$$

when M = DLHρ, and $\bar{V}$ is the average relative velocity of the control volume segment with respect to V_p. Since the acceleration of the control volume is expected to be small the term

$M(\frac{d\bar{V}}{dt})/g_c$ may be neglected. Noting that

$$\frac{dM}{dt} = \frac{dD}{dt} LH\rho \quad , \tag{12}$$

and

$$\bar{V} = \frac{1}{2} \left(\frac{dD}{dt}\right) \quad , \tag{13}$$

we obtain the result

$$F_m = \frac{1}{2g_c} \left(\frac{dD}{dt}\right)^2 LH\rho \quad . \tag{14}$$

In deriving the term F_i, F_b and F_m it has been assumed that the density front velocity similarity profile is that shown in Fig. 3. Thus, to account for the fact that the actual velocity profile may be different from that assumed (i.e., $\bar{V}$ may not simply equal

$$\frac{1}{2} \left(\frac{dD}{dt}\right)$$

the parameter γ is introduced as follows:

$$\left(\frac{dD}{dt}\right)_{\text{Actual}} = \gamma \left(\frac{dD}{dt}\right) \tag{15}$$

where

$$\left(\frac{dD}{dt}\right)_{\text{Actual}}$$

is the actual rate of growth of the distance D defined in Fig. 3. The entire equation of motion may now be written as

$$\frac{\beta}{2} LH^2 \Delta\rho \frac{g}{g_c} = \frac{f_i}{g_c 8} \rho\gamma^2 \left(\frac{dD}{dt}\right)^2 D \cdot L$$

$$+ \frac{f_b}{g_c 8} \rho \left(\frac{\gamma}{2} \left(\frac{dD}{dt}\right) V_p - \frac{\gamma^2}{4} \left(\frac{dD}{dt}\right)^2\right) D \cdot L$$

$$+ \frac{\gamma^2}{2g_c} \left(\frac{dD}{dt}\right)^2 LH\rho \tag{16}$$

The above equation is quadratic in $\frac{dD}{dt}$, with the solution being

$$\frac{dD}{dt} = \frac{-\gamma F_b V_p D_p \pm \sqrt{\frac{(\gamma F_b \rho V_p D)^2}{8} + 4\beta H^2 \Delta\rho g\left(\frac{\gamma^2 f_i}{4}\rho D - \frac{\gamma^2 f_b D}{16} + \gamma^2 H\rho\right.}}{2\left(\gamma^2 \frac{f_i}{4}\rho D - \frac{\gamma^2 f_b \rho D}{16} + \gamma^2 H\rho\right)} \quad (17)$$

Now if typical values of the various parameters are used to evaluate Eq. (17) ($\gamma = \beta = 1$) it becomes apparent that the effect of V_p, for the range of Foude numbers of interest, is small. Thus, the terms containing V_p can be neglected in Eq. (17). Equation (17) is then simplified to the form

$$\frac{dD}{dt} = \alpha\left[\frac{H^2\Delta\rho g}{H + \left(\frac{f_i + f_b/4}{4}\right)\rho D}\right]^{1/2} \quad (18)$$

where $\alpha = \beta/\gamma^2$.

Thus, the expression for the rate of growth of the horizontal projection of the interface is given by an equation with a single free parameter to be determined by experiment. The total velocity of the leading edge of the density front is now expressed as

$$V_f = C_o V_p + \frac{\alpha}{2}\left[\frac{H^2\Delta\rho g}{H\rho + \left(\frac{f_i + f_b/4}{4}\right)\rho D}\right]^{1/2} \quad (19)$$

The displacement of the leading edge at time t from D = 0 at t = 0 is

$$X_f = C_o V_p t + \frac{1}{2} D(t) \quad (20)$$

where D(t) is obtained by integrating $\frac{dD}{dt}$ Eq. (18) from time-zero to time-t. The resulting expression for D(t) is

$$D(t) = \frac{4H^2\Delta\rho g}{\rho(f_1 + f_b/4)}\left[\left(\frac{\rho}{H\Delta\rho g}\right)^{3/2} + \left(\frac{3\rho(f_i + f_b/4)}{8H^2\Delta\rho g}\right)(\alpha T)\right]^{2/3} - \frac{4H}{(f_i + f_b/4}} \quad (21)$$

The position of the trailing edge at time t would be

$$X_t = C_1 V_p t - \frac{1}{2} D(t) \quad (22)$$

Since no specific assumption has been made regarding the exact density-induced velocity distribution, the above equation only predicts the position of the leading edge or trailing edge of the density front. The parameters C_o and C_1 correct for the fact that the channel velocity at the height of the leading edge (or trailing edge) is, in general, different from the mean plug-flow velocity. The values C_o and C_1 can be determined by assuming that the unperturbed velocity profile in the pond is given by the relationship [4]

$$V(y) = V_s \left(\frac{y}{y_o}\right)^{1/6} , \quad (23)$$

where V_s is the surface velocity. Strictly speaking, the value of C_1 would always be zero since the no-slip condition always holds at fixed boundaries. However, since the present interest is in the bulk flow behavior it was sufficient to assume that

$$C_o - 1 = 1 - C_1 \quad (24)$$

The case of the advancing cold front presents a different problem. In this case the maximum density-induced forward velocity occurs near the bottom of the channel. The position of maximum density-induced forward velocity is not coincident with the position of maximum forward velocity of the unperturbed channel flow as in the case of the advancing hot front, due to the no-slip bottom boundary condition.

The advancing cold front case thus represents a more desirable situation than with the advancing hot front in terms of achieving a near vertical density front velocity profile. In view of this fact no effort has been made to quantify the behavior of the advancing cold front other than to say that for TSP design purposes the advancing hot front is the more restrictive design condition. This conclusion has been verified by experiment.

Results of Initial Design Concept Evaluation

Based on the initial design concepts three prototype TSPs have been designed to span the range of design densimetric Froude numbers from 0.5 to 1.5. Three model designs which simulate these prototype designs were tested in the flume. All three designs result in unsatisfactory thermal hydraulic performance of the pond.

All three of the TSP designs summarized in Table 1 have significant density-induced flows which partially reduce the pond thermal capacitance. The highly unstable inlet flow jets were successful in establishing initially a nearly vertical density front. However, as the density front propagates a short distance downstream from the inlet mixing region significant vertical stratification begins to develop. In fact, except for the case of a densimetric Froude number of 1.5, the trailing edge of the density front was not observed to travel a significant distance beyond the inlet mixing region. A short time after the initiation of the inlet flow, the overlying hot wedge is somewhat diluted as a result of inlet flow mixing. This small dilution nevertheless is rapidly overcome by the continuing intrusion of the unmixed inlet flow, and a distinct density interface develops rapidly.

Accurate visual determination of the position of the trailing edge of the upper fluid layer in all cases was difficult since in none of the experiments was the inlet flow able to displace rapidly or to mix with the initial cold water in the boundary layer at the bottom of the channel. Figure 4a shows qualitatively the profile of the density front for F_D greater than about 1.00. The interface is nearly linear except at the leading and trailing edges. At lower densimetric Froude numbers density front profiles developed as shown approximately in Fig. 4b.

In addition to the three experimental runs performed at densimetric Froude numbers of 0.5, 1.0 and 1.5 several runs were made at higher densimetric Froude number values to see if any gross changes in the flow behavior would occur. In all cases the flow behavior was observed to remain qualitatively unchanged.

The positions of the leading edge of the advancing density front as a function of time for each of the TSP designs of Table 1 are shown in Fig. 5. In each case the position is plotted in a non-dimensional manner as a function of the fraction of the plug-flow residence time V/Q, which had elapsed. The design parameters are equal for all of the ponds except for the densimetric Froude number values. As Fig. 5 indicates, even a TSP with a Froude number of 1.5 (which corresponds to a channel only 72 feet wide and 15 feet deep for a typical set

of design parameters) is observed to short-circuit long before the plug-flow residence time has elapsed. Clearly, this problem becomes worse at even lower design densimetric Froude number values. Once the density front has reached the withdrawal region, the pond would be effectively short-circuited since selective withdrawal of the remaining cold layer is not possible.

A total of eight experimental runs were made to determine the value of the empirical constant α of Eq. (19). In each experimental run the position of the advancing hot front was observed visually and recorded as a function of time, and all of the resulting data points are plotted in Fig. 6. The coordinate axes in Fig. 6 are chosen such that the slope of the straight line drawn through the data points is equal to the empirical coefficient α. The abscissa variable is time, while the ordinate variable is the result of integration of Eq. (19), followed by solution for αT. The ordinate variable is

$$y^* = \frac{1}{C} \left(\frac{D+E}{A}\right)^{3/2} - \frac{B}{C} \quad , \tag{25}$$

where

D = observed position of the leading edge of the advancing hot front at time t,

$$A = \frac{4H^2 \Delta\rho g}{(f_i + f_b/4)}$$

$$B = \left(\frac{\rho}{H\Delta\rho g}\right)^{3/2} ,$$

$$C = \frac{3}{8} \frac{\rho}{\Delta\rho} \left(\frac{f_i + f_b/4}{H^2 g}\right), \text{ and}$$

$$E = \frac{4H}{f_i + f_b/4} \quad .$$

An approximate best-fit straight line was drawn through each set of data points, and a value of α determined. The average value of α is 1.09. Using this value of α, the data points for all 8 experimental runs can be predicted with an average error of 4.0%. The average error for the run with the poorest agreement is 7.2%.

Evaluation of Design Modifications

As has been indicated previously, an efficient and economical horizontal plug-flow TSP cannot be designed as envisioned in the initial design concept. If the development of the TSP design on the basis of a horizontal plug-flow pond were to be pursued then some measures had to be taken to retard the advancing density front, and the resultant TSP short circuiting. Thus, some simple modifications of the initial design concept have been investigated by testing the effects of design changes in the experimental model.

There appear to be two different means of retarding the density-induced flow in a TSP. The first is simply the correct placement of barriers in the pond such that the advance of the leading edge of the front is retarded. The second is the placement of barriers in the pond such that internal mixing jets are created which have the effect of reducing the local density differences, and consequently of retarding any density-induced flow. Actually, any barrier or constriction placed in the pond will have, to varying degrees, both of the above effects. Any constriction produces a jet as a result of the locally increased flow velocity, and a barrier will retard the leading edge of either a hot or cold advancing front. Thus, the design task has been to select empirically an appropriate pond constriction design and to determine the required number of such constriction in order to yield the desired result of adequately diminishing the density-induced flow short-circuiting.

Performance of Barriered Ponds

Initially a determination of the relative merits of horizontal versus vertical barriers was made. A horizontal barrier is of the type shown in Figs. 7a and 7b while a vertical barrier would have the general characteristic of blocking the entire width of the pond over a part of the water depth.

As is shown in Fig. 8, the horizontal barrier concept was found to be superior. Figure 8 compares the thermal capacitance performance of identical ponds (except for barrier geometries) on the basis of percentage of the theoretical cooling potential recovered from the pond as a function of time. The time variable is plotted in a non-dimensional manner by dividing by the plug-flow residence time V/Q where V is the pond volume and Q equals the flow rate. Mathematically, the percentage of the theoretical cooling potential recovered, R(t) is defined as follows:

$$R(t) = 100\% \int_0^t \frac{T_i - T_{oa}}{T_i - T_{ot}} \cdot \frac{d\tau}{(V/Q)} \qquad (26)$$

where

T_i = pond inlet temperature,

T_{oa} = actual outlet temperature,

T_{ot} = outlet temperature for theoretical plug-flow, and

t = elapsed time of operation

Also shown in Fig. 8 is the idealized plug-flow performance curve and the performance curve for a TSP with no flow constrictions.

All the curves in Fig. 8, except that for the idealized plug-flow case, are deduced from actual temperature measurements in the model at the point of flow withdrawal. Correction was made for water surface heat loss from the flume based on an experimental determination of the water to air heat transfer rate.

The performance curves in Fig. 8 indicate that in maintaining the total amount of flow constriction constant at 1/2 the total cross-sectional area (i.e., constant barrier pressure drop) the horizontal barriers appear to be slightly more efficient than the vertical barrier. If one considers the comparative difficulty in construction the vertical barrier, the horizontal is also seen to be the more desirable option.

At least two processes appear to be contribution to the vertical mixing of the hot and cold fluids. The first process in the downward movement of the hot upper layer along the upstream surface of the barrier, followed by streaming around the barrier and through the constriction. Passing through the constriction is an apparently nearly homogeneous flow which in the second process mixes with the ambient water in the downstream pond segment. However, the mean temperature of the flow through the constriction is necessarily less than that of the upstream hot layer since the underlying cold layer is gradually drawn through the constriction. The same processes occur at succeed-barriers downstream. In fact, succeeding barriers are more efficient in mixing the stratified layers since the density front at each succeeding barrier is progressively less stable than previously.

Refinement of Horizontal Barrier Concept

In attempting experimentally to optimize the design of a barriered TSP two general problems needed investigation. The first is the design of the barrier itself, and the second is the specification of the number and spacing of barriers required to obtain good pond performance. Beyond these two problems the tradeoffs between decreasing the pond design densimetric

Froude number value, and increasing the number of barriers was investigated. Additionally, the effect of a floating roof was evaluated.

Horizontal barrier design variation from that shown in Fig. 8 include different total area constrictions, and a distribution of the constriction over the width of the channel such that multiple smaller internal jets would be created at each barrier. Increasing the total constriction (i.e., more blockage of flow) has the advantage of creating more vigorous jet mixing. However, the experiments have shown that decreased jet size may lead to undesirable preferential attachment of the jet to the pond wall resulting in partial short-circuiting. The phenomenon, termed the Coanda effect, is similar to that occurring in bistable fluidic switching devices. In the TSP model this effect was observed at a design $F_D = 0.5$, and a barrier geometry at 5/6 total constriction with a 1/6-width slot at the center of the pond. In this case the jet issuing from the first barrier became attached to the pond wall, bypassing a large part of the pond volume between the barriers. A large recirculating eddy was formed in each segment as is shown in Fig. 9. The result of this behavior is that no increase in the pond performance was noted beyond that obtained in the case of a 1/2 total area constriction. This attachment effect appears to be adequately counteracted by using smaller multiple jets to obtain the same total flow constriction.

Several experiments were performed to examine the effect of varying pond length of the number of barriers required to achieve a certain level of performance. The results are summarized in Table 2. Essentially, these results indicate that the number of barriers required to achieve a certain level of performance (percent of the theoretical cooling potential recouped at the plug-flow residence time V/Q) may be largely independent of the length (storage volume) of the pond. To see this, compare the results of case 1 to those of cases 2 and 3 in Table 2. Intuitively this conclusion can be related to the need in the smaller (shorter) ponds to diminish the density induced flow more quickly than in the larger (longer) ponds. One would also expect that there would be a diminishing rate of return for the addition of barriers to the pond. Such behavior has been observed, as is shown in Fig. 10.

As in the case of the unbarriered TSP the tendency for short-circuiting was observed to increase with decreasing design densimetric Froude number value in the case of the barriered pond. Decreasing the design densimetric Froude number value allows for a deeper and wider pond, but to maintain high performance additional (or more effective) barriers need to be added. Table 3 gives the performance loss for a decrease in

design densimetric Froude number from 0.5 to 0.25 (cases 1 and 2). However, in comparing cases 1 and 3 in Table 3 it is apparent that a highly efficient pond can still be realized with the same number of barriers by increasing the effectiveness of the barriers. The barrier effectiveness is increased by increasing the total constriction, which in turn increases the jet mixing effect.

In addition to the modeling of the behavior of the advancing hot front at the design condition temperature difference of 10°F, experimental runs were made to examine the off-design behavior. One run was made which is identical to case 1 in Table 2 except that instead of a hot discharge into a cold pond, cold water was discharged into an initially hot pond. This simulates the "cooldown" mode of operation. As anticipated the performance increased from 87% to 92% (percentage of theoretical cooling potential recouped at $T = V/Q$). Also as anticipated an evaluation of the off-design performance ($\Delta T = 5°F$ for a TSP of the same design revealed an increase in the performance from 87% to 90%.

Summary and Conclusions

The two basic options for the design of a thermal storage pond for use with a dry cooling tower — horizontal and vertical plug-flow — have been evaluated with regard to their value in TSP applications. The horizontal plug-flow pond was selected for detailed evaluation based on its relative merits. Subsequently, an initial design concept was formulated for the horizontal plug-flow pond and its performance evaluated by the use of an experimental model. The result was found to be unsatisfactory due to the magnitude of the density-induced flows. Thus, modification of the initial design concept was required. Various flow constriction which induced flow mixing were evaluated in model studies in order to determine their relative merits. A simple full-depth barrier with vertical slot jets proved to be a very successful in achieving control of the density-induced currents.

Experiments were performed to examine the sensitivity of the pond performance to variations in the design densimetric Froude number, and to the number and geometry of the flow constrictions. In addition off-design performance was evaluated.

The main conclusion of this design investigation is that a horizontal plug-flow thermal storage pond of apparently reasonable geometry and cost can be designed such that the ideal plug-flow behavior is approximated well. The following TSP specification results in the excellent design-condition performance shown in Fig. 11. This case may be used to evaluate TSP

construction costs:*

Design F_D = 0.25,
Depth = 20 ft.,
Width = 240 ft.,
No. of barriers = 8
Length = (dependent on desired storage volume),
Barrier geometry = 5/6 total constriction, horizontal type, 3 slot,
Discharge structure = 10 uniformly spaced 4 ft. dia. submerged nozzles,
Withdrawal structure = no specific structure required, and
Cover = (floating cover will enhance performance).

It should be emphasized that many other designs may also prove to be efficient thermally, and may ultimately be more economical. Qualitatively, tradeoffs between the above parameters may be made on the following basis:

Increasing design F_D value results in improved TSP performance,

Increasing depth results in degraded TSP performance,

Increasing width results in degraded TSP performance,

Increasing number of barriers results in improved TSP performance, and

Increasing total barrier constriction results in improved TSP performance.

*For design flow = 1000 cfs, design $\Delta T = 10°F$

REFERENCES

1. Guyer, E.C. and Golay, M.W., "An Engineering and Economic Evaluation of Some Mixed-Mode Waste Heat Rejection System," Department of Nuclear Engineering, Mass. Inst. of Tech. Report MITNE-191, 1976.

2. Jirka, G., Abraham, G., and Harleman, D.R.F., "Assessment of Techniques of Hydrothermal Prediction," Ralph M. Parsons Laboratory for Water Resources and Hydrodynamics Report #203, MIT, 1975.

3. Abraham, G., "Magnitude of Interfacial Shear in Exchange Flow," Journal of Hydraulic Research, 9, 1971, No. 2.

4. Rohsenow, W., and Choi, H., Heat, Mass, and Momentum Transfer, Prentice-Hall, New Jersey, 1961.

TABLE 1

THERMAL STORAGE POND MODEL DESIGNS

		Case 1	Case 2	Case 3
1.	Densimetric Froude Number	1.5	1.0	.50
2.	Depth (inches)	4.5	4.5	4.0
3.	Width (inches)	18	18	18
4.	Aspect ratio	0.25	0.25	0.22
5.	Mean Velocity (ft/sec)	0.28	0.19	0.088
6.	Total flow (GPM)	70.4	47.2	19.5
7.	Reynolds Number	30,000	20,100	8,830
8.	Scale factor	48.4	72.7	147.0
9.	Temperature difference (°F)	40	40	40
10.	Vertical Distortion	1.21	1.80	3.33
11.	$\frac{f_o(1/D)\ \text{model}}{f_o(1/D)\text{prototype}}$	1.83	1.38	0.94
12.	Discharge	highly unstable submerged multiport		

TABLE 2

EXPERIMENTS TO EXAMINE EFFECT OF NUMBER OF BARRIERS ON POND PERFORMANCE

Case	F_D	Number of Barriers	Prototype Storage Volume	Percentage of Total Theoretical Cooling Potential Recovered at t/(V/Q)=1.0
1	0.5	8	6	87%
2	0.5	4	3	81%
3	0.5	8	3	89%

All barriers 1/2 total area constriction, 3 slot horizontal type

TABLE 3

EXPERIMENTS TO DETERMINE EFFECT OF
DESIGN DENSIMETRIC FROUDE NUMBER ON
TSP PERFORMANCE

Case	F_D	Number of Barriers	Fraction of Cross-Sectional Area blocked by Barrier	Percentage of Total Theoretical Cooling Potential Recovered at t/(V/Q)=1.0
1	0.5	8	1/2	87%
2	0.25	8	1/2	75%
3	0.25	8	5/6	86%

All barrier horizontal type, 3 slot, Prototype Storage Volume = 6 hrs.

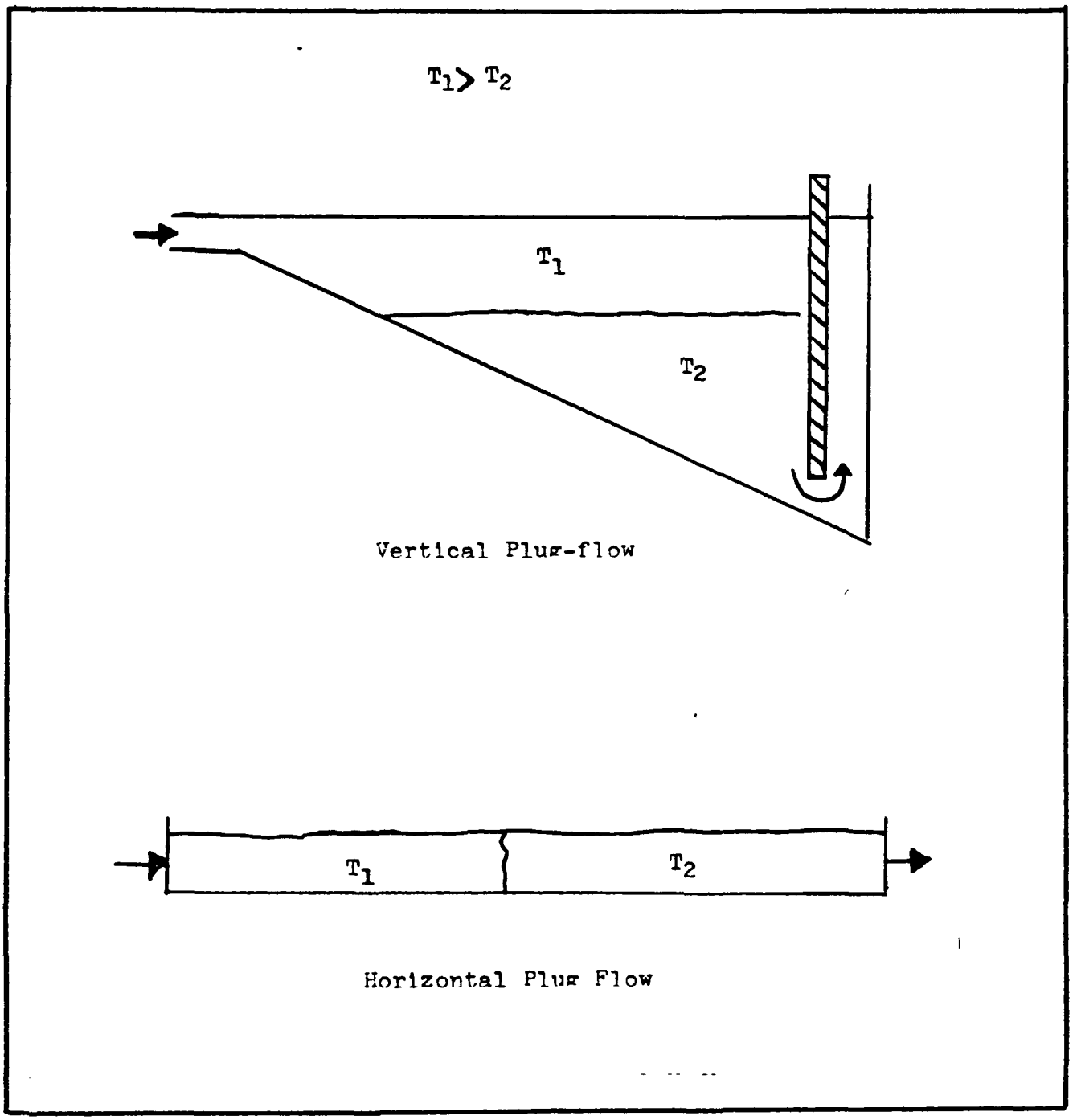

Fig. 4.1 Horizontal and Vertical Plug-Flow Concepts

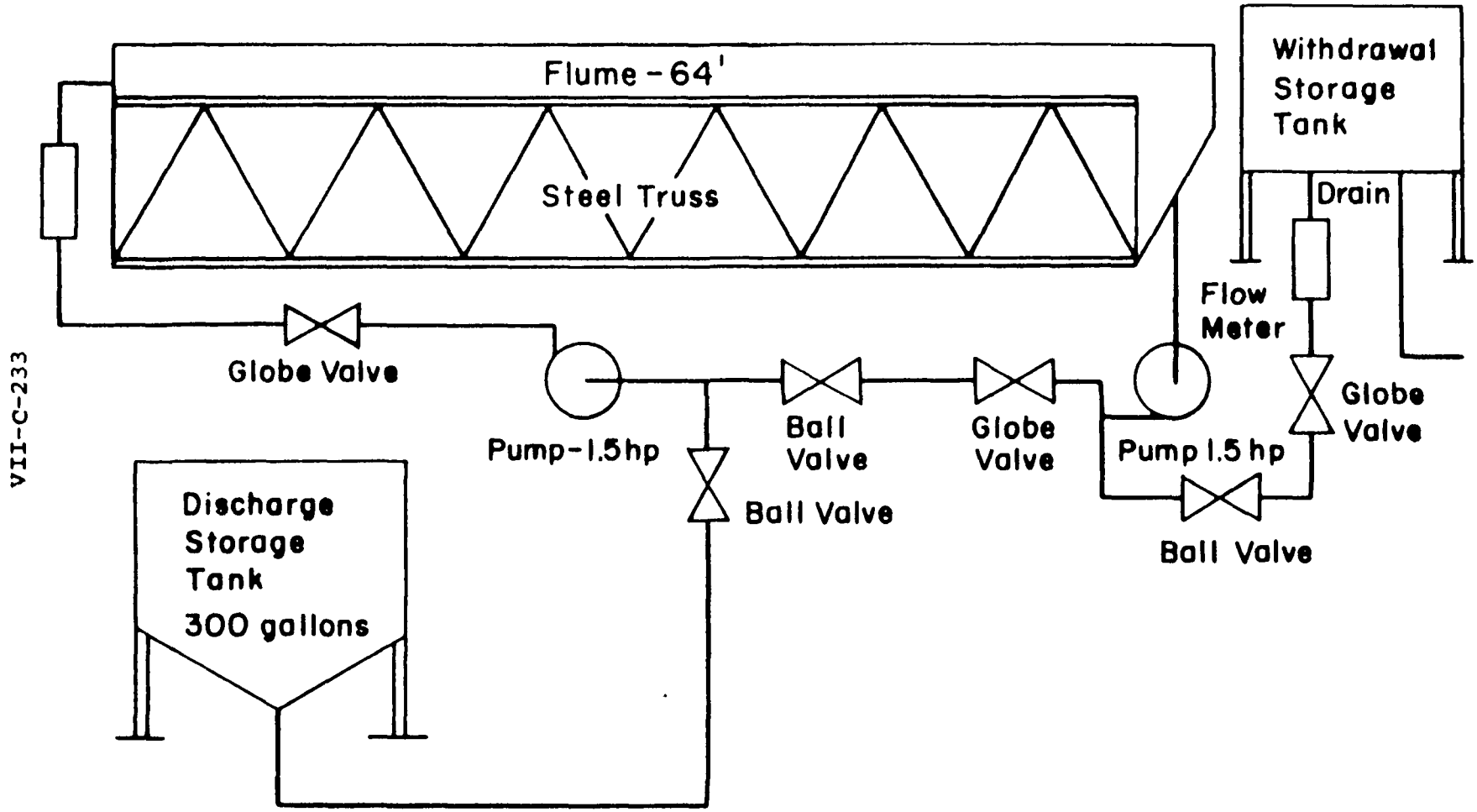

Fig. 4.7 Schematic of Thermal Storage Pond Model Experiment

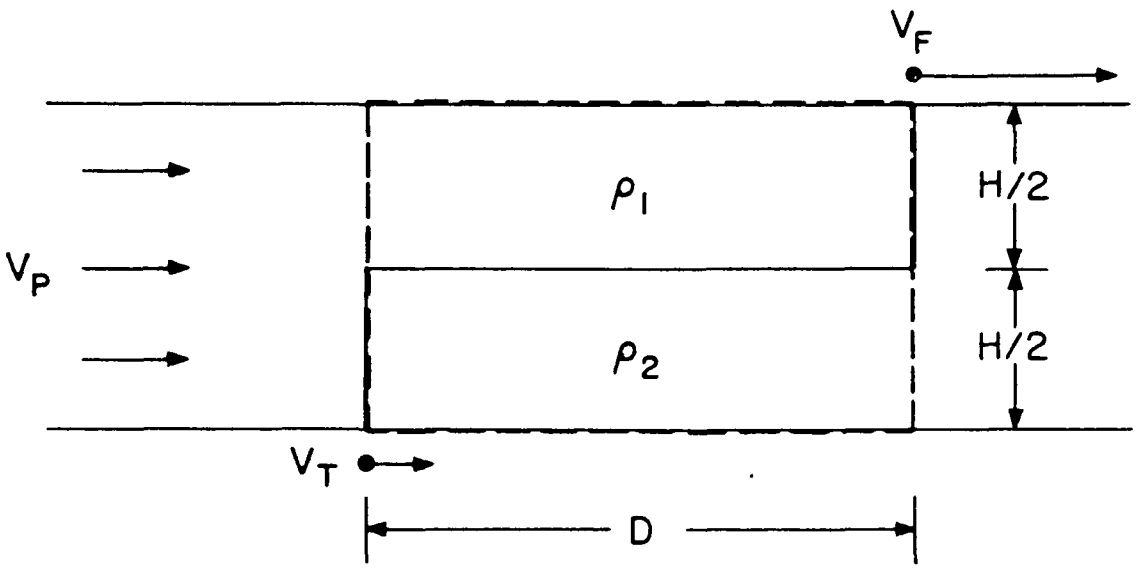

Fig. 4.8 Density -Induced Flow Control Volume

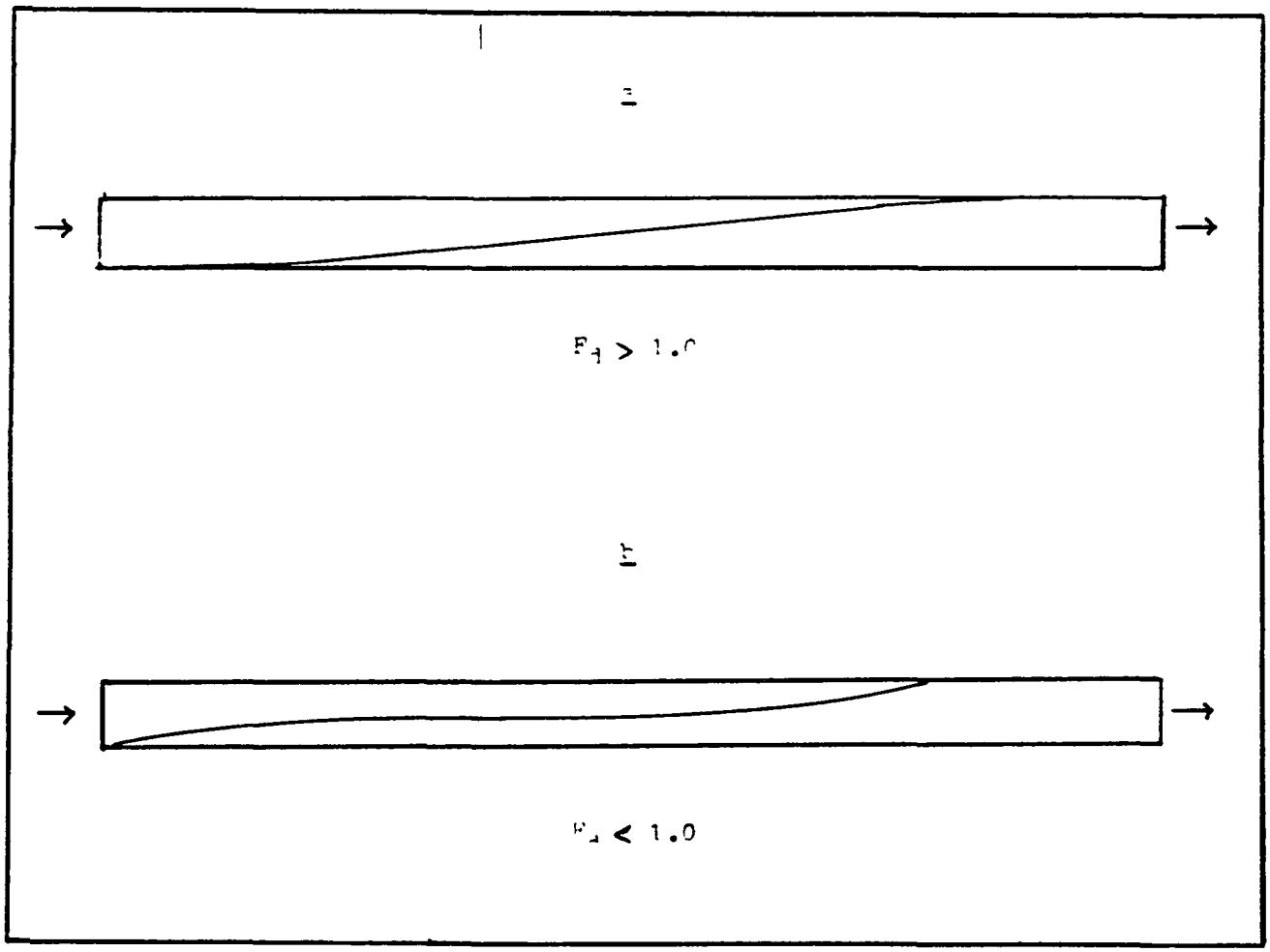

Fig. 4.10 Illustration of Density Front Profile - Advancing Hot Front

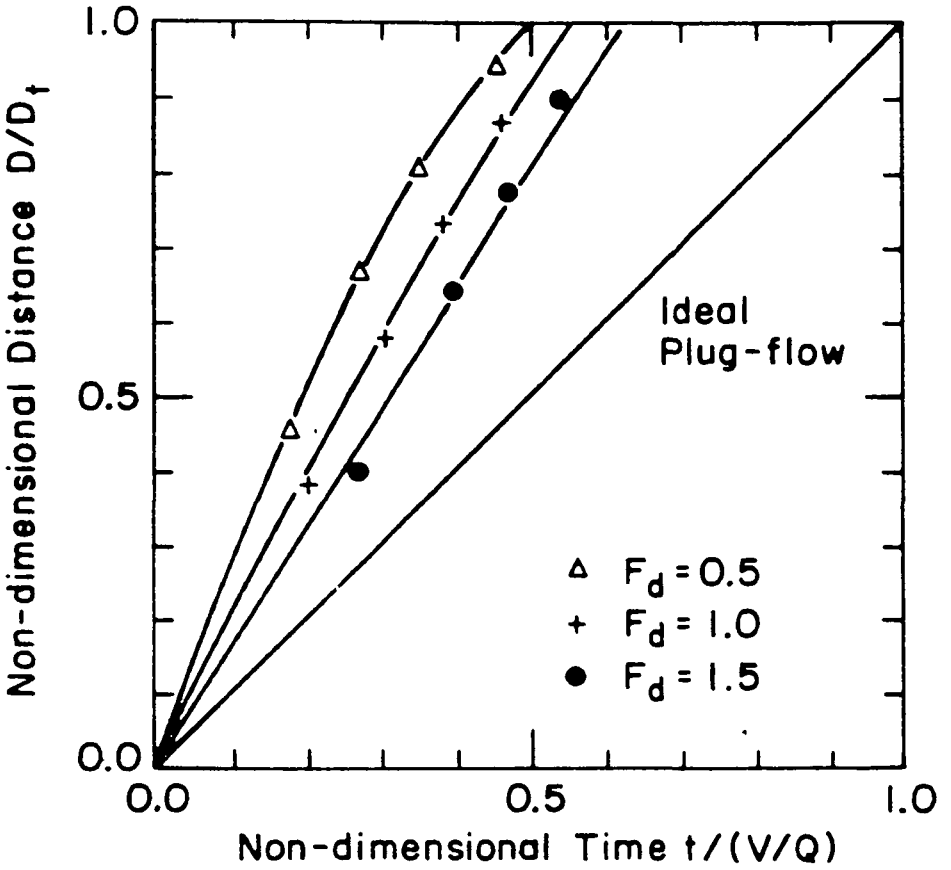

D = Actual Position of Leading Edge of Density Front

D_t = Total Lenght of Pond

Fig. 4.11 Propogation of Density Front as a Function of TSP Design Densimetric Froude Number

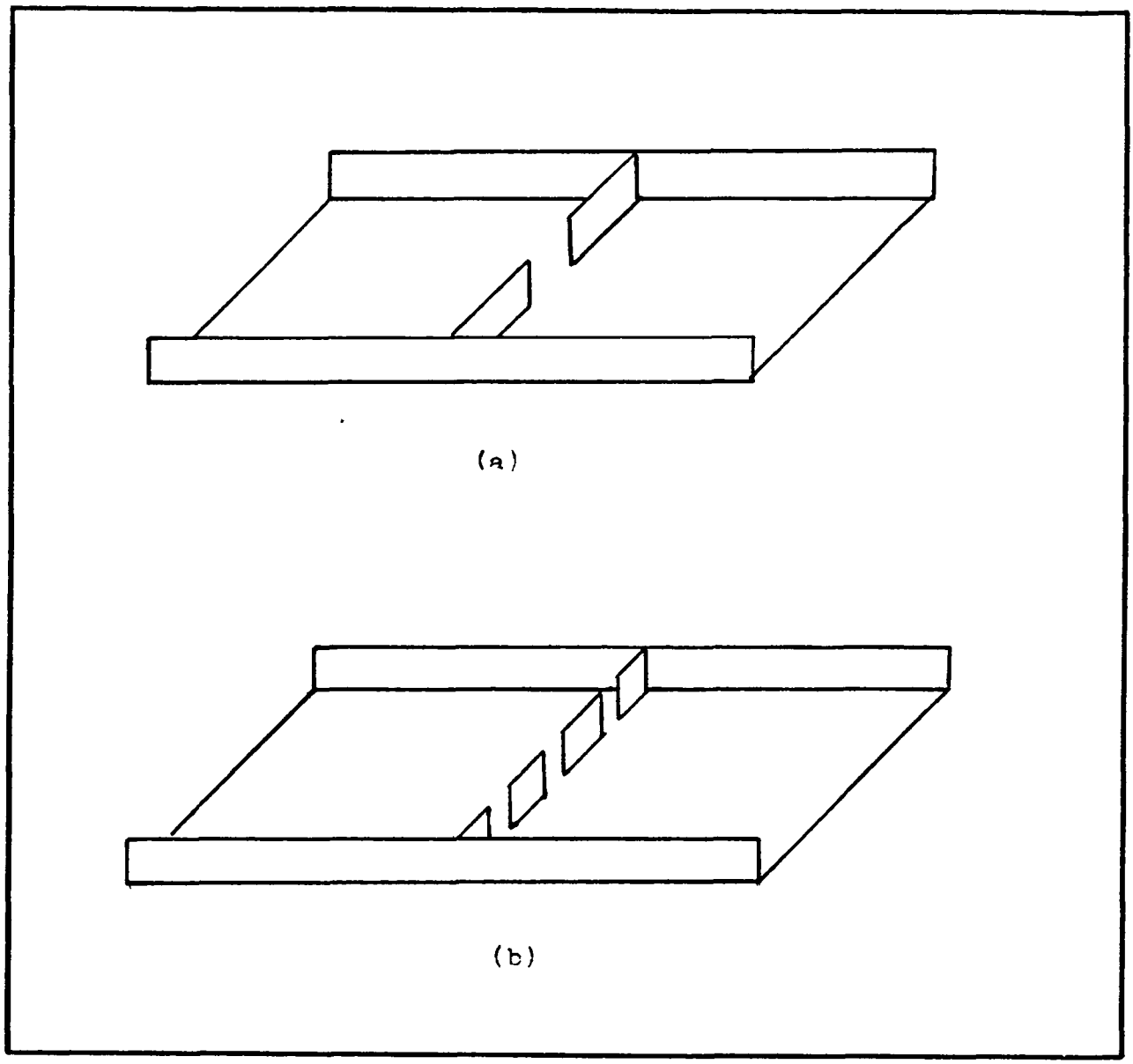

Fig. 4.17 Horizontal Barriers

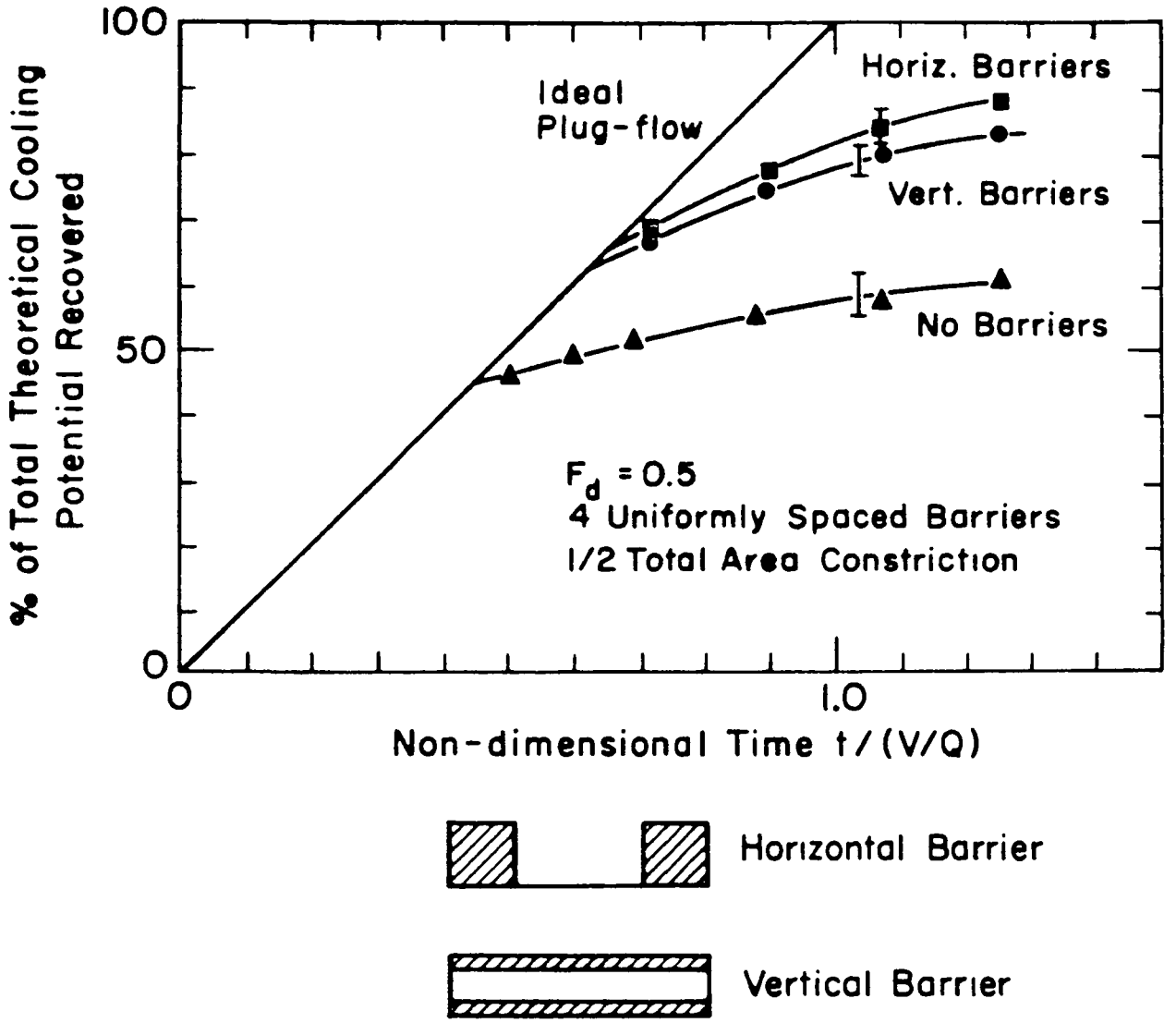

Fig. 4.19 Performance of Barriered TSP

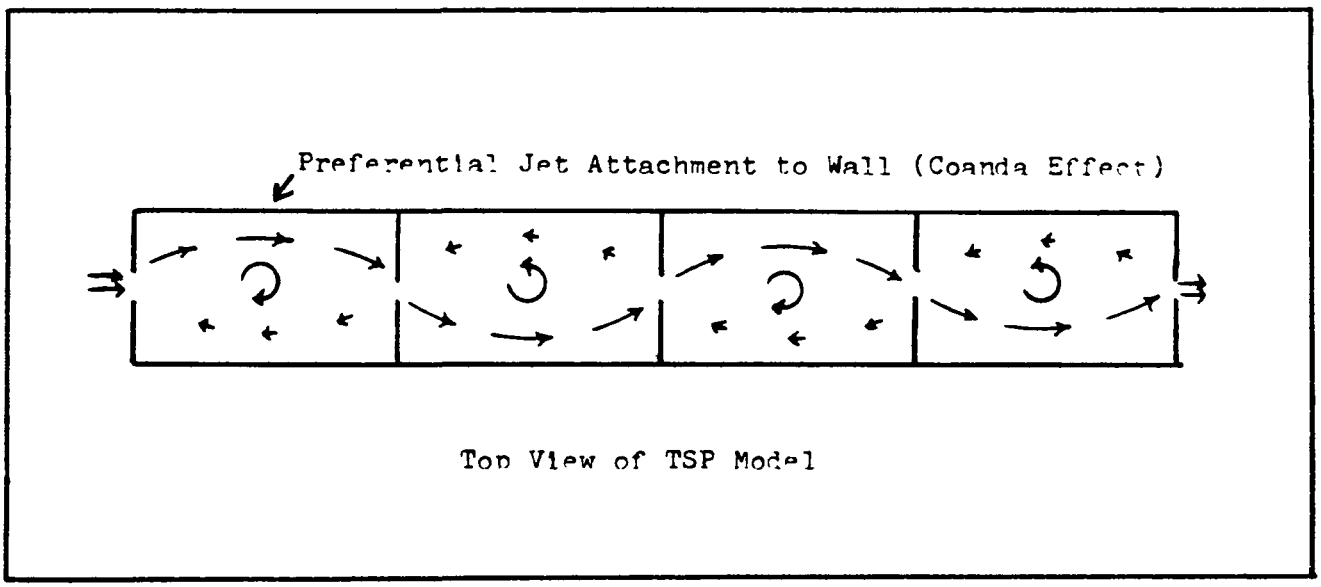

Fig. 4.20 Flow Field Resulting From Attached Jet

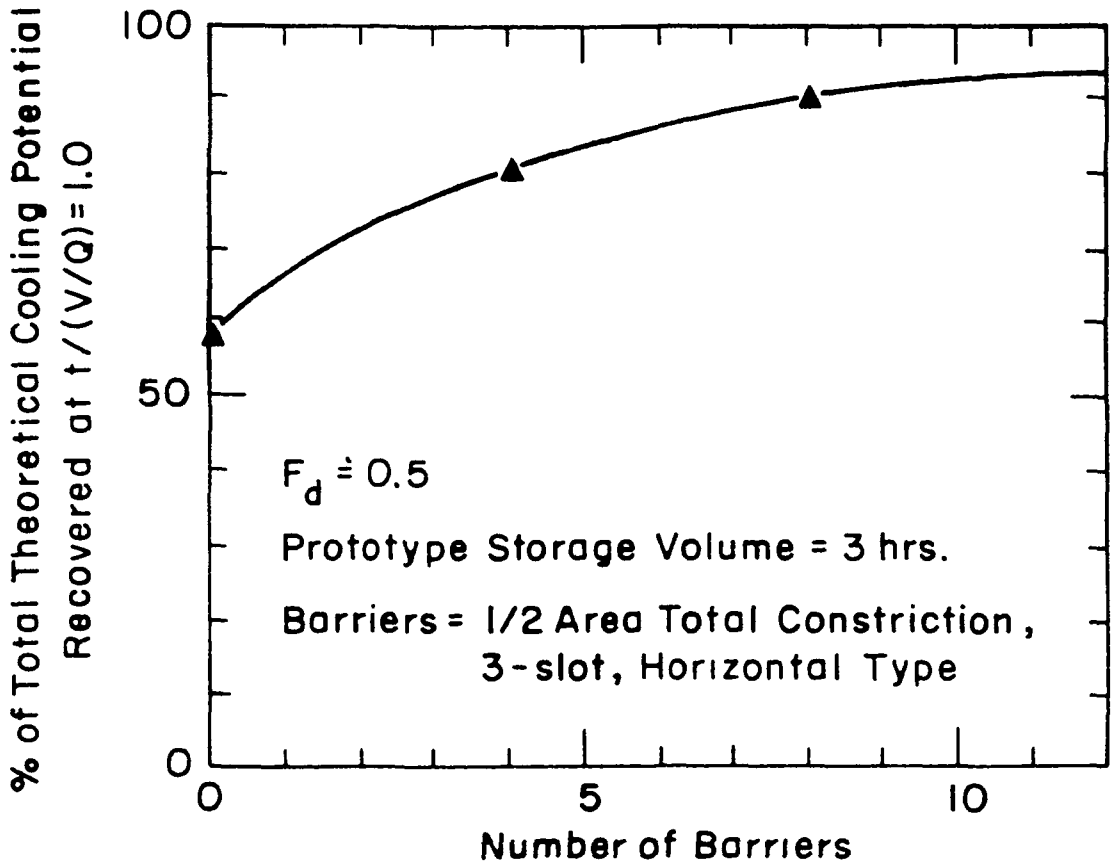

Fig. 4.21 TSP Performance as a Function of the Number of Barriers

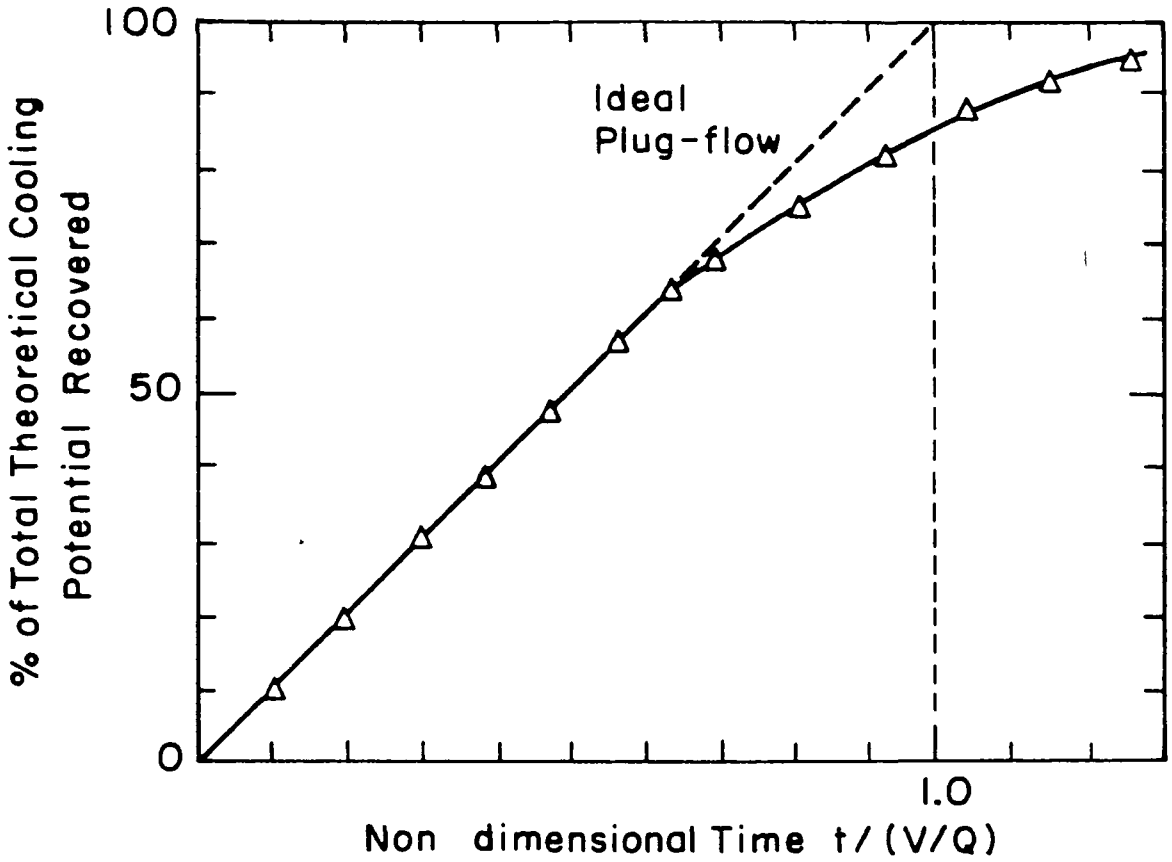

$F_d = 0.25$

Prototype Storage Volume = 6 hrs.

Barriers = 8, 5/6 Total Area Constriction
3-slot, Horizontal Type

Fig. 4.30 Performance of Recommended Design

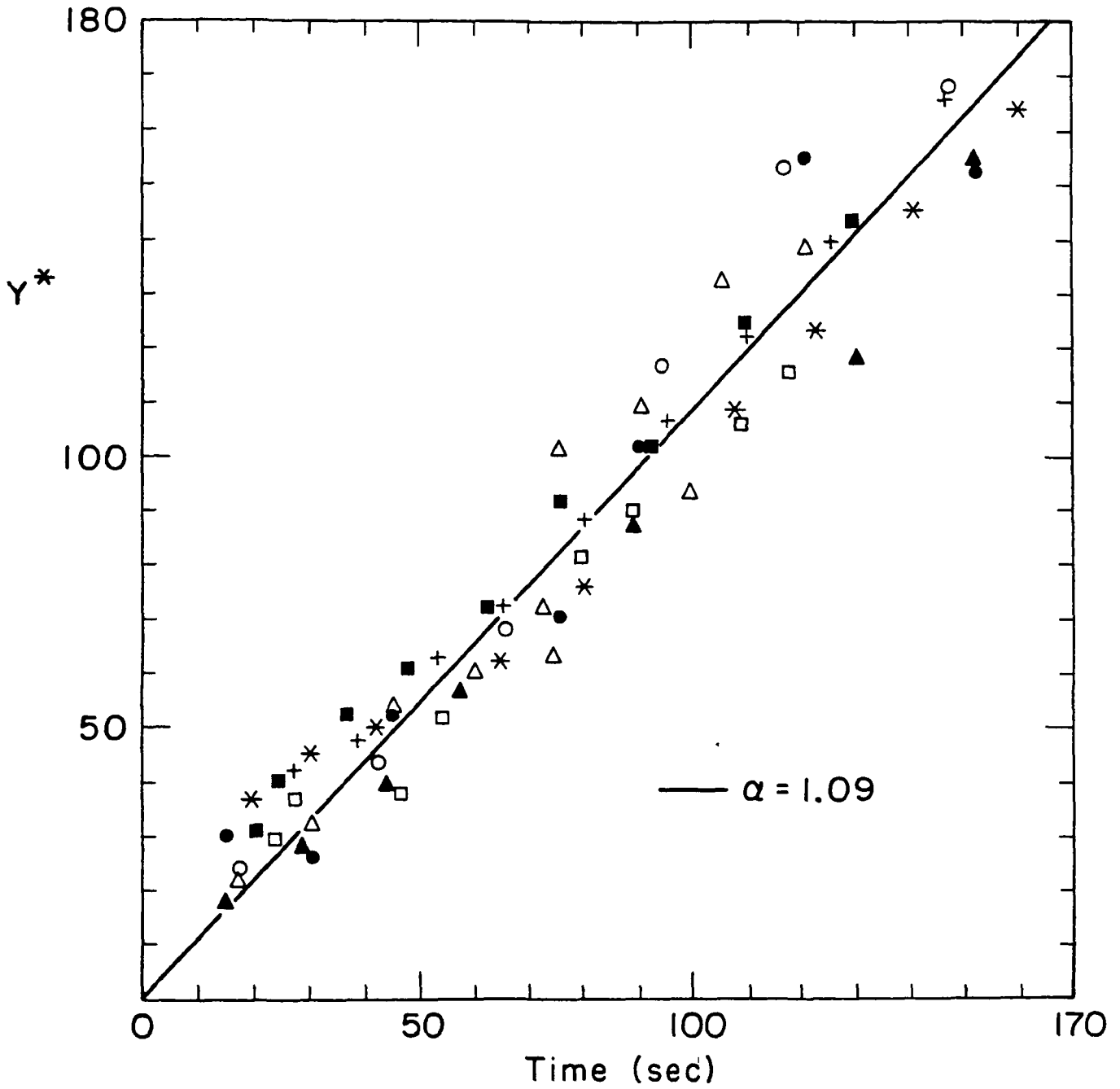

Fig. 4.12 Data for α Determination